

Selective Hardening in E52100 Steel

F.W. Giacobbe

A process involving the use of an argon thermal plasma jet to facilitate selective hardening of a high-carbon steel (E52100) has been studied experimentally. Cylindrical hollow specimens (approximately 8.0 cm OD by 6.0 cm ID by 9.0 cm long) were treated during this process by rapidly heating the central section of these samples to 870 °C, soaking at 870 °C for 1.0 to 2.0 min and then rapidly quenching the samples. All samples were continuously turned at an angular velocity of about 6 rev/sec during each trial run to promote uniform changes in temperature. A noncontact infrared sensor was also used to monitor and facilitate specimen temperature control throughout the heating and soaking phases of each test trial. The heat treated specimens were sectioned longitudinally, polished, and used to obtain microhardness profiles for several of these heat treated specimens. This work indicated that complete and relatively uniform through hardening was achieved in all of the test specimens. A significant advantage of this process over other more conventional hardening methods involves the very rapid heat transfer rates that are possible between a plasma jet flame and the heated object. An additional and somewhat related advantage is that undesirable overheating of specimen sections (adjacent to the heat treated zone) by conduction can be minimized. This effect may permit the production of selectively hardened steel objects that cannot be produced using more conventional technology.

1 Introduction

THE E52100 grade of high-carbon steel is made in relatively large quantities by the electric furnace process.[1] This type of steel serves in many important commercial applications due to its strength, wear resistance, and extremely high hardenability.[2] Typically, these properties are optimized by austenitizing at 845 to 860 °C in a neutral salt bath or in a gaseous atmosphere with a carbon potential near 1.0%, followed by an oil quenching process.[3] After quenching, parts are usually tempered at 160 to 180 °C to convert tetragonal martensite to cubic martensite.[4]

Generally, hundreds of identical parts are simultaneously heat treated and then tempered as indicated above. However, one drawback of this process is that the entire part is affected and, thus, hardened. In some objects, this is undesirable because a portion of these parts must be clamped, bolted, or otherwise secured within or on some other structural component. Often, the secured portion of these parts does not have to be hardened and, thus embrittled, in these areas, which are especially prone to fatigue-type failure mechanisms.[5-8] In some special cases, this problem can be significantly reduced by selective hardening. One way to achieve this is to rapidly heat only the portion of a particular part that must be hardened above the 845 °C austenitizing temperature. Then, rapid quenching will cause only this portion of the part to fully harden. One relatively new method of executing this type of selective hardening process involves the use of a high-temperature plasma jet heating system.[9] This process has been used, in the past, to study selective hardening in a 1095 grade of high-carbon steel.[10] Due to the commercial importance of the E52100 grade of high-carbon steel, a similar and more extensive experimental study involving this type of steel was also undertaken. The purpose of this article is to describe the experimental results of this most recent study.

F.W. Giacobbe, Chicago Research Center/American Air Liquide, Inc., Countryside, Illinois.

2 Apparatus

2.1 *Overview*

The thermal plasma jet heater used during this study was a much larger version of a similar device used to study selective hardening in small-diameter cylindrical solid and hollow specimens made from a 1095 grade of carbon steel.[10] Due to several unique design features in this thermal plasma heating system and its potential utility in other applications, this system has been described in detail.

A detailed drawing of the large-scale plasma jet heat source (torch) may be seen in Fig. 1. A cross-sectional top view of the plasma jet furnace enclosure, as well as a specimen support and rotation mechanism, may be seen in Fig. 2. The primary aim of these drawings is to show overall system dimensions, as well as system component dimensions.

2.2 *Cathode*

The materials of construction used to fabricate the cathode were copper tubing (K-type), solid copper (free machining), brass, and thoriated tungsten in the cathode tip. Standard, threaded brass, compression-type fittings were also used in the cathode and elsewhere. A stainless steel, quick-disconnect (MDC, DC-112, MDC Vacuum Products Corp., Haward, CA), welded internally into the stainless steel support flange (MDC, F458000), was used to position and hold the cathode in place during system operation.

2.3 *Plasma Gas Injection Ring*

The plasma gas injection ring was machined from a solid cylindrical piece of Teflon. The gas entry port was angled to provide tangential gas injection. This feature produces a swirling or vortex gas flow around the cathode and through the arc discharge region. The lower pressure at center of the vortex and between the cathode tip and anode tends to permit the formation of a very stable plasma arc. The plasma gas injection ring was also machined with the same bolt hole pattern as the stain-

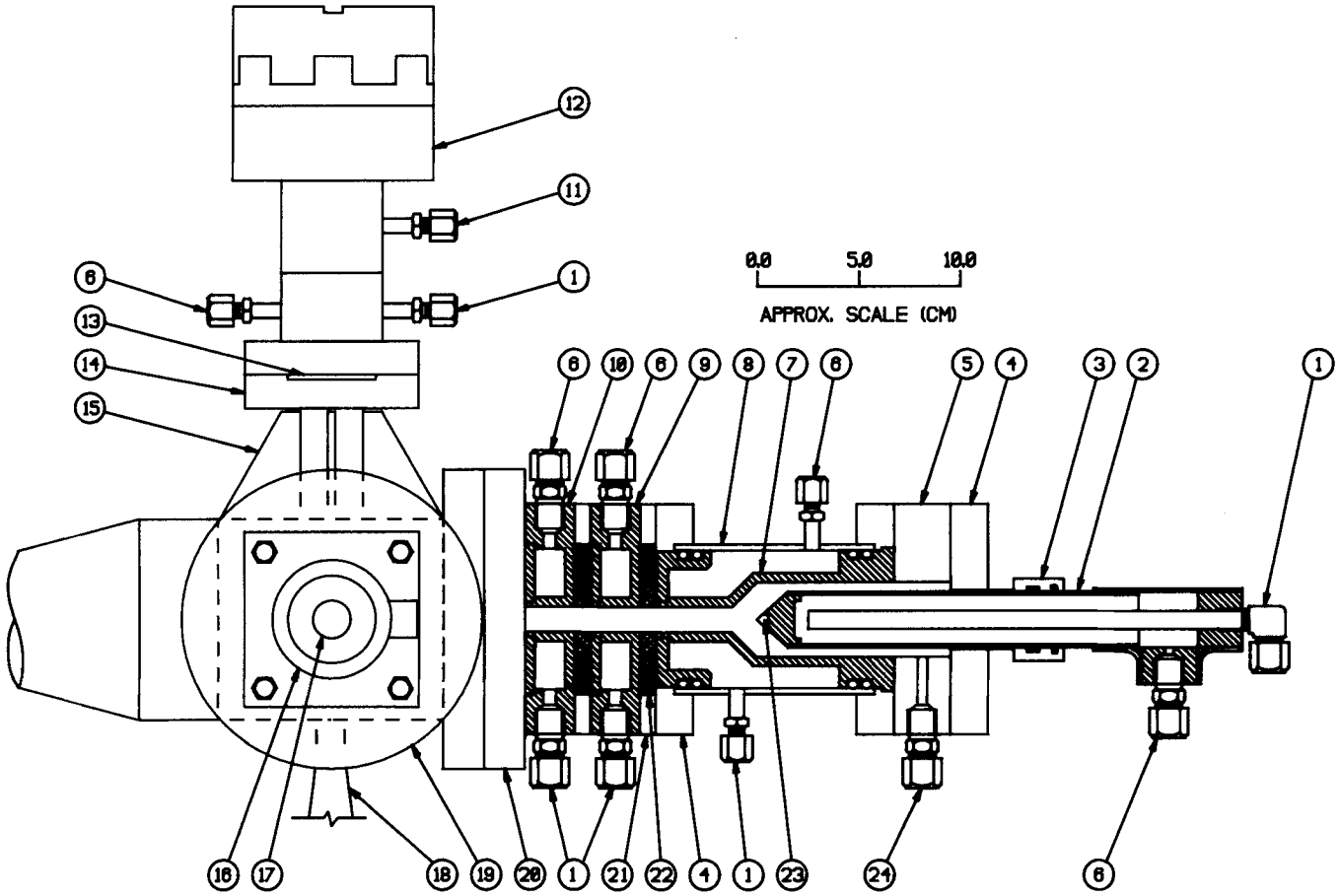

Fig. 1 Thermal plasma jet heating system. (**1**) Water inlet. (**2**) Cathode. (**3**) Cathode sealing ring. (**4**) Cathode support flange. (**5**) Plasma gas injection ring. (**6**) Water outlet. (**7**) Cathode enclosure. (**8**) Water jacket. (**9**) Wall stabilization ring. (**10**) Anode. (**11**) Gas purge inlet. (**12**) IR temperature sensor. (**13**) Sliding door assembly. (**14**) IR sensor support flange. (**15**) Stainless steel gusset. (**16**) High-temperature bearing. (**17**) Specimen support rod. (**18**) Quenchant inlet. (**19**) Flange-furnace door. (**20**) Coupling flange. (**21**) Teflon insulator. (**22**) Ceramic insulator. (**23**) Tungsten insert. (**24**) Plasma gas inlet.

less steel flanges (MDC, F458000 and F458300) bolted onto each of its sides. To insulate (electrically) the cathode from other downstream metallic components, the plasma gas injection ring was bolted between the stainless steel flanges (mentioned above) with nylon bolts and nuts. A gastight seal was made with rubber gaskets and/or a silicone sealant material.

2.4 *Cathode Enclosure*

The cathode enclosure was machined from a solid cylindrical piece of copper. A pair of O-ring grooves was cut into each end of this component to seal it into its water-cooled jacket. The water-cooled jacket was made from a section of 7.62 cm OD stainless steel pipe. Each end of this pipe section was socket welded into a stainless steel flange (MDC, F458300).

2.5 *Wall Stabilization Ring*

The wall stabilization ring was machined from a solid cylindrical piece of brass. The water-cooled cavity, within this component, was enclosed by silver soldering a round flat section of the same type of brass on one side of the wall stabilization ring. This component extends the arc distance between the cathode and anode. Therefore, a higher operating voltage is required between the cathode and anode. This feature permits a higher power input to the plasma arc without a corresponding increase in arc current. Additional wall stabilization rings are also possible, provided the available power supply is capable of instigating plasma ignition across a wider gap between the electrodes.

2.6 *Anode*

The anode was identical to the wall stabilization ring. The main difference between the anode and the wall stabilization ring is related to their behavior during system operation. Specifically, because arc termination occurs at the plasma anode, the heat load that this component must endure is substantially greater than the heat load experienced by the wall stabilization ring. Quantitative measurements regarding this behavior have been published in the past.[11]

The anode, insulating spacers, and wall stabilization ring were bolted between the cathode enclosure jacket and a stainless steel reducing flange (MDC, 600 by 458 cm) leading into the plasma jet furnace enclosure. The bolts holding this part of

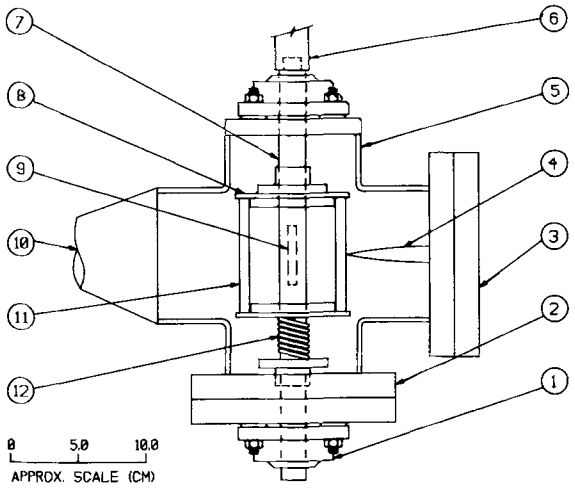

Fig. 2 Furnace enclosure. (1) High-temperature bearing. (2) Flange-furnace door. (3) Coupling flange. (4) Plasma jet "flame." (5) Stainless steel cross. (6) Rotational coupling. (7) Specimen support rod. (8) Specimen support collar. (9) Quenchant inlet. (10) To vent and drain. (11) Cylindrical specimen. (12) Spring-compression.

the system together were also insulated to isolate (electrically) the anode from the wall stabilization ring.

2.7 *Gas Purge Inlet*

The gas purge inlet port provided a means of permitting a low flow of an inert gas to sweep particulates, generated during system operation, away from the optical surfaces within the infrared (IR) temperature sensor.

2.8 *Infrared Sensor*

The IR sensor (Transtemp 1500) was manufactured by the Williamson Corp. (Concord, MA). This device has been described in detail in a previous publication.[10]

2.9 *Sliding Door Assembly*

The sliding door assembly was machined from a flat plate of stainless steel. The purpose of this component was to protect the optics in the IR sensor from the coolant fluid injected onto the heat treated cylinders immediately after plasma processing.

2.10 *High-Temperature Bearings*

High-temperature bearings (Dodge, 11-124060) were used to permit the specimen support rod to rotate freely during plasma processing. These bearings were bolted against the front flange and to the back of the high-temperature furnace enclosure.

2.11 *Specimen Support Rod*

The specimen support rod was machined from solid stainless steel cylindrical bar stock. This component was used to support the cylindrical specimens that were heated by the argon plasma jet. Additional details regarding the specimen support rod may be seen in Fig. 2.

Table 1 Approximate Coolant Flow Rates

Component	Flow rate, l/hr
Cathode	380
Cathode enclosure	380
Wall stabilization ring	265
IR sensor	265
Anode	300

2.12 *Quenchant Inlet*

The quenchant inlet was fabricated from stainless steel plate stock. This component was TIG welded into the bottom of the large stainless steel cross used as the primary component of the plasma furnace enclosure. The quenchant inlet port was intentionally elongated (see Fig. 2) so that the high flow (*i.e.*, about 190 l/min) of quenchant would be directed evenly over a wide band on the heated metallurgical specimens.

2.13 *Large Flanges*

A large, solid stainless steel flange (MDC, F600000) was used on the furnace enclosure as a door. A hollow, but otherwise nearly identical stainless steel flange (MDC, 600400), was used to mechanically couple the plasma jet generator to the high-temperature furnace enclosure. One of these flanges (the reducing flange) had a bolt hole pattern that matched the pattern on the smaller cathode support flange.

2.14 *Teflon Insulators*

Cylindrical Teflon insulators were machined from flat stock and installed on both sides of the wall stabilization ring. These insulators were also machined with a bolt hole pattern that was identical to the pattern on the cathode support flange.

2.15 *Ceramic Insulators*

Ceramic insulators were machined from flat stock Macor.[12] These high-temperature insulators were installed inside the Teflon insulators.

3 System Operation

3.1 *Plasma Jet Torch*

The plasma jet torch was typically operated at electrical power input levels between 8 and 30 kW, depending on the desired ramping rates and soaking temperatures. Operating voltage and current requirements were in the range of 80 to 120 V and 100 to 250 A.

The main plasma gas used during this work was pure argon, although a few experiments involving the use of argon/helium mixtures were also carried out. Plasma gas flow rates were typically 160 SLPM at STP (standard liters per minute at 1

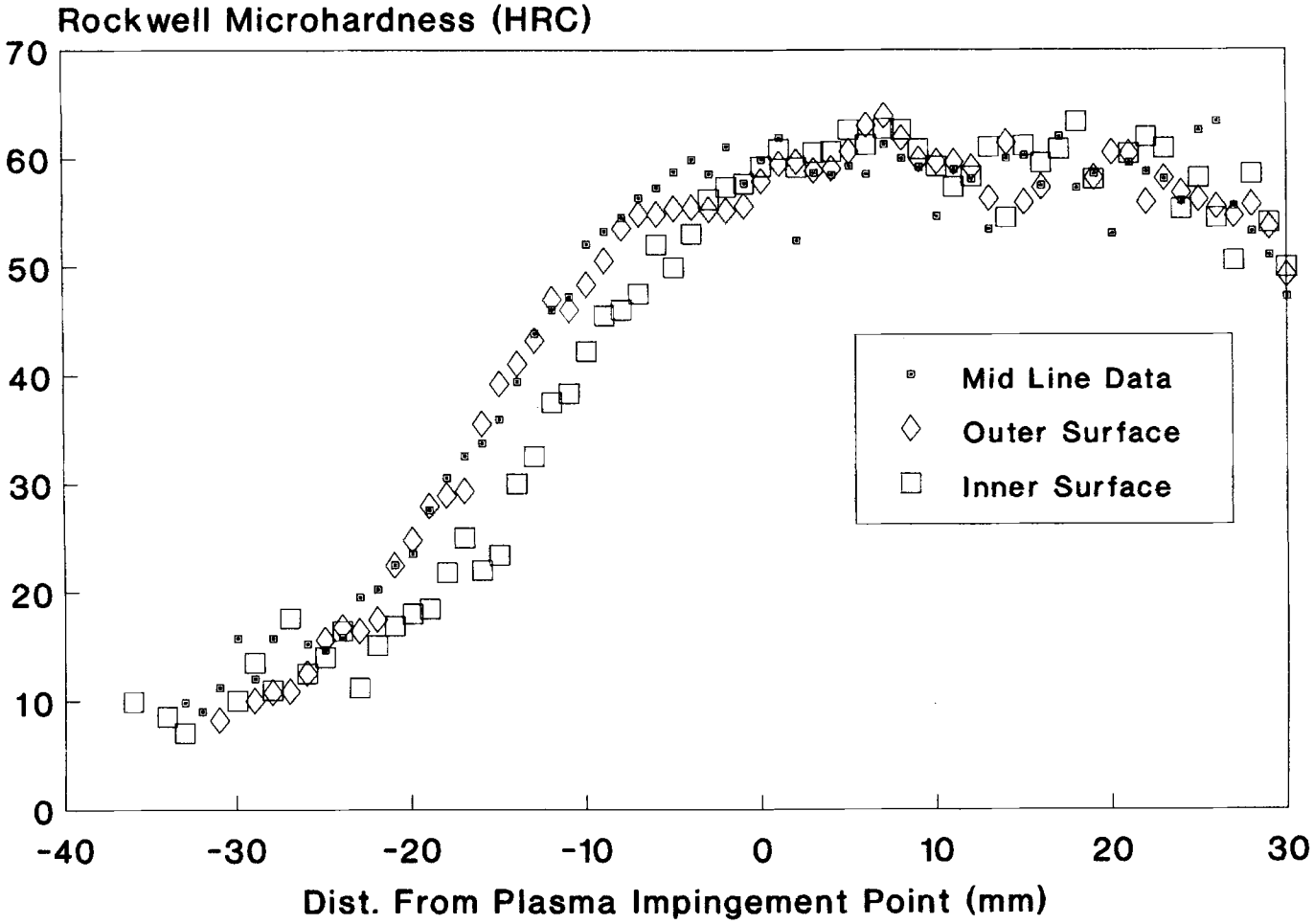

Fig. 3 Axial microhardness profiles of Sample No. 1.

atm, 0 °C). Pure argon was also used to purge the optical path between the heated specimens and the IR sensor. This flow rate was typically about 10 SLPM at STP.

The cathode, cathode enclosure, wall stabilization ring, anode, and base of the IR sensor were all water cooled. Coolant flow rates through these components are listed in Table 1.

3.2 *Furnace Enclosure*

Specimens to be heated were individually mounted on the specimen support rod. Then, the specimen support rod was placed in the furnace enclosure and supported by the two high-temperature bearings mounted on the front and back of the furnace (see Fig. 2). The mounted specimens were continuously turned at an angular velocity of about 6 rev/sec to ensure even circumferential heating by the argon plasma jet.

3.3 *Infrared Sensor*

During specimen heating, the IR sensor was used to monitor the surface temperature of the rotating hollow cylinders. This device was coupled to a digital indicator that provided instantaneous temperature readings. In addition, the IR sensor signal was used to produce a permanent analog record of temperature versus time behavior for each heated sample. The analog record was also used as a guide to assist in controlling sample heating rates and soaking times at elevated temperatures. This control was exercised by manually varying the plasma arc current during the heating process.

3.4 *Metallurgical Specimens*

All of the metallurgical specimens used during this study were fabricated from a single section of heavy-wall E52100 steel tubing. These specimens were all machined into identical hollow cylinders. The dimensions of these cylinders were approximately 8.0 cm OD by 6.0 cm ID by 9.0 cm long. Prior to each trial run, the individual cylindrical specimens were mounted on the specimen support rod and then placed within the high-temperature furnace enclosure (see Fig. 2).

3.5 *Specimen Quenching*

To produce the desired metallurgical structure within the plasma-heated specimens, they had to be rapidly quenched. This process caused (primarily) the formation of a martensi-

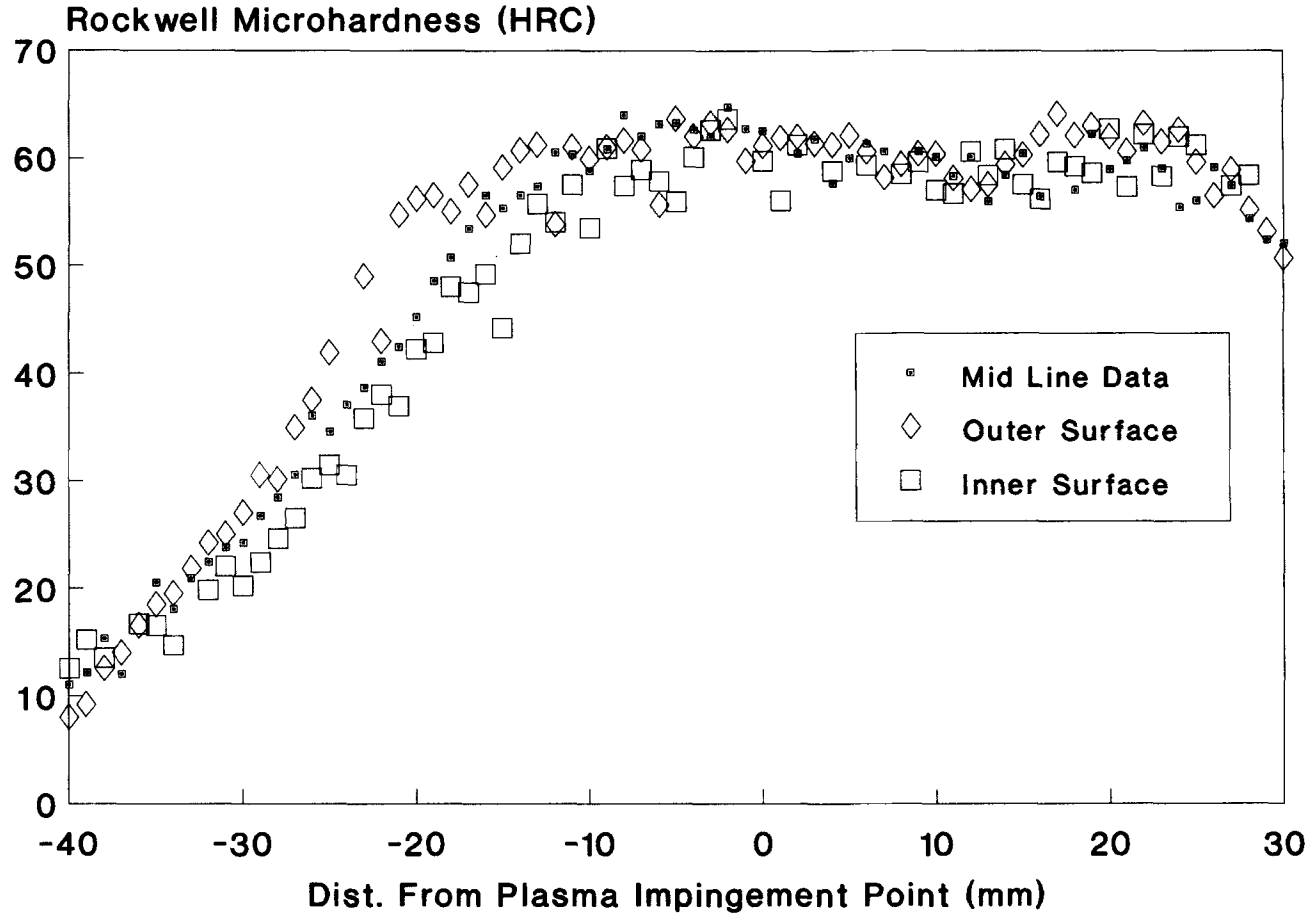

Fig. 4 Axial microhardness profiles of Sample No. 4.

Table 2 Sample Operating Parameters

Parameter	Sample No. 1	4	5	6
Time taken to reach 870 °C(a), min	5.4	10.9	8.2	6.0
Time held at 870 °C, min	1.0	1.0	2.0	1.0
Total run time, min	6.4	11.9	10.2	7.0
Avg current/voltage requirements during preheat to 870 °C(b), A/V	210/110	190/88	190/88	180/84
Quenchant flow rate, l/min	26	26	26	190

Note: All plasma gas flow rates were ~135 SLPM throughout each trial run. **(a)** This variable was partially dependent on residual quenchant fluid trapped in the system after the previous quenching step. **(b)** The plasma power required to maintain sample specimens at 870 °C was typically 11.5 kW during all trial runs.

tic[13] structure within the directly heated band of specimen material. Due to the intentional asymmetric heating and quenching of the plasma-heated specimens, one end of these objects remained relatively soft after the heat treating/quenching process was completed. There was also a narrow region, between the very hard and relatively soft regions, of transitional hardness in the heat treated specimens.

Because of the large size and mass of the heated specimens, the quenching rate (*i.e.*, quenching fluid impingement rate) had to be very high. This fluid quenching rate was about 190 l/min. This high fluid flow rate was produced by two large gear type pumps (Gorman, RGS1) coupled together in parallel and each powered by a 2 hp, 220 VAC, three-phase electric motor. The pumping assembly was mounted on a platform bolted to the top of a 210 l reservoir of the quenchant fluid. Immediately after heating of the specimens was terminated, the pumping system was manually activated. A piping system (from the quenchant reservoir, to the gear pumps, and then to the quenchant inlet port of the plasma furnace enclosure) directed the quenchant fluid through the quenchant inlet port and onto the hot (typi-

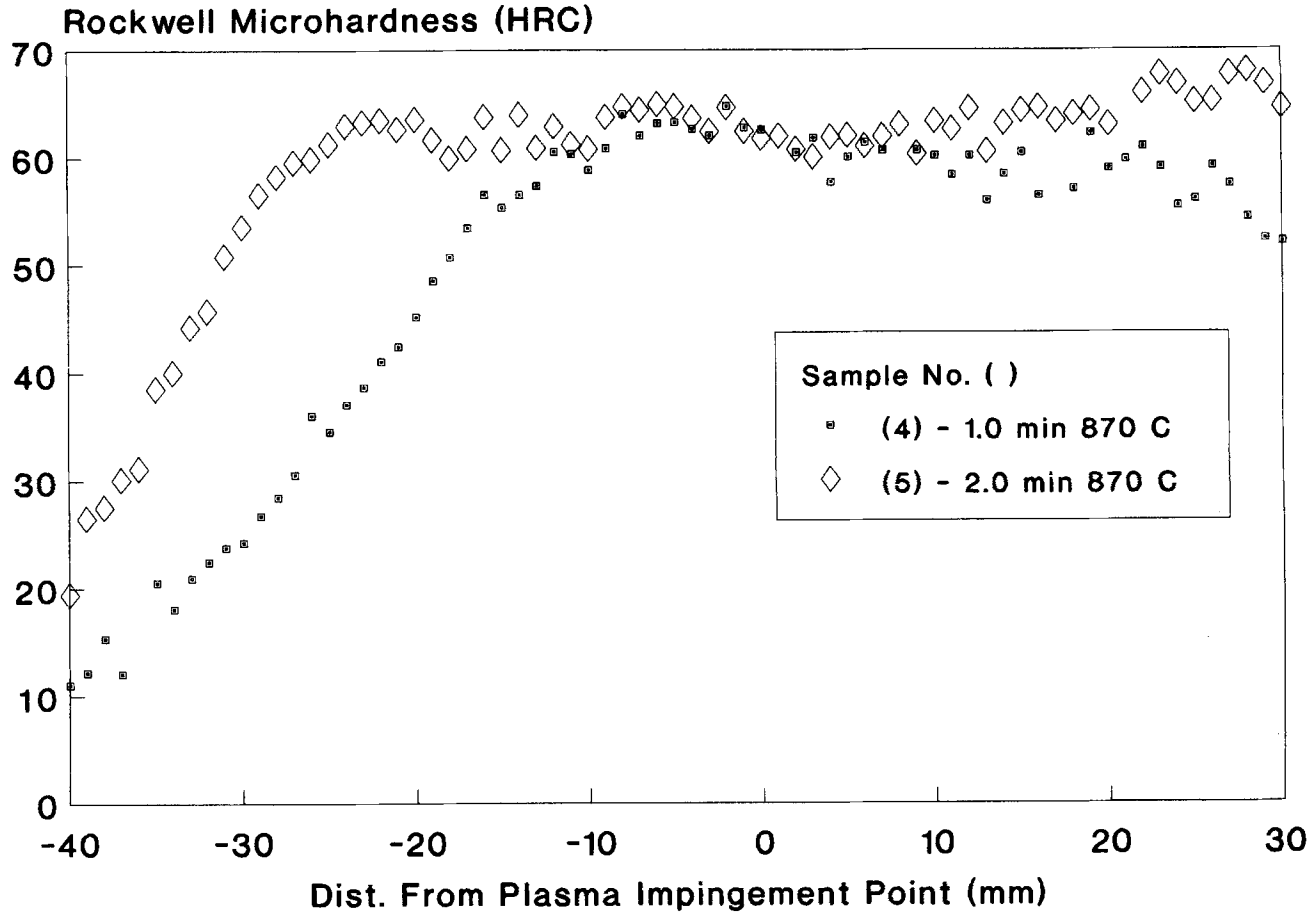

Fig. 5 Axial microhardness profiles of Sample No. 4 and 5 from mid-line data.

cally about 870 °C) rotating specimen. The spent quenchant fluid was collected in a large reservoir, after exiting the furnace enclosure, and automatically (by gravity) returned through a 5.1 cm ID pipeline to the quenchant reservoir. Due to the large volume of this fluid, there was only a nominal increase in its temperature after each trial run.

4 Examples of Experimental Results

Over a dozen separate hollow cylindrical specimens were heat treated using the thermal plasma jet system described above. However, only four of these specimens (No. 1, 4, 5, and 6) are discussed below to exemplify some of the results that were obtained. The results obtained after processing the first of these four specimens are summarized in Fig. 3. Several details regarding the treatment of, and results related to, this specimen should be clarified. In particular, this specimen (as well as all others discussed herein) was intentionally heated asymmetrically, *i.e.*, the center of the plasma "flame" was directed at a circumferential line on this specimen that was about 60 mm from one end and only 30 mm from the other end. This part was also heated from room temperature to 870 °C in 5.4 min, then held at 870 °C for 1.0 min just prior to quenching. In addition, a relatively low quenchant fluid flow rate (*i.e.*, 26 l/min) was used to cool this part after heating. This quenchant fluid entered a circular port (approximately 9.5 mm ID) located directly below the heated circumferential line on the rotating specimen. Only later, when the use of this method of cooling (as well as the quenchant fluid flow rate) was deemed to be insufficient, was the system modified as described earlier in this article.

The Rockwell microhardness readings plotted in Fig. 3 should also be explained. Specifically, these readings were obtained using a pyramidal diamond point hardness tester (Leco, Model M-400, microhardness tester). The metallurgical specimen used in the microhardness tester was cut (longitudinally) out of the heat treated ring using a water-cooled abrasive cutting wheel. The midpoint readings were taken along a longitudinal line directly through the center of this specimen (*i.e.*, this line was parallel to the axis of the heated cylinder and had a radius exactly between the outer and inner radius of the original cylindrical specimen). The outer surface readings were also taken along a parallel longitudinal path, but were located only 1.0 mm below the outer surface of the sectioned specimen. The inner surface readings were taken similarly, but were located 1.0 mm above the inner surface of the sectioned specimen. Because the original specimens were cooled by quenchant impingement directed only at their outer surfaces, these three separate sets of hardness measurements were taken to document how the quenching and cooling technique actually af-

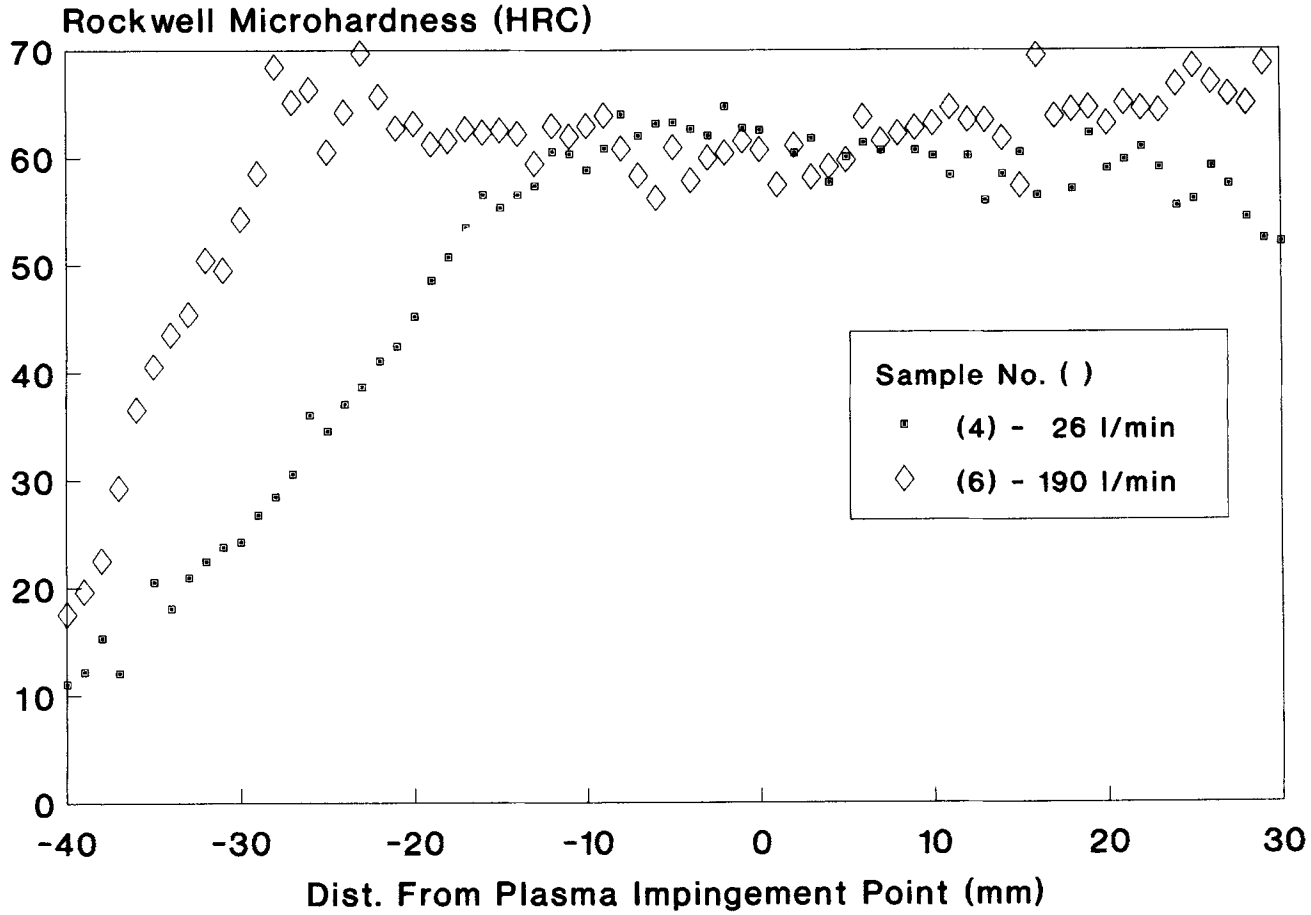

Fig. 6 Axial microhardness profiles of Sample No. 4 and 6 from mid-line data.

fected the radial (and longitudinal) hardness of the finished steel specimens.

It is obvious that there is some scatter in the microhardness data plotted in Fig. 3. However, the overall hardness trends are clear. In particular, sample specimen No. 1 remained fairly soft at one end and very hard at the other. In fact, the actual hardness (~60 HRC) at the hardened end is very near the typical maximum hardness that can be achieved in this type of steel (*i.e.*, ~64 HRC[14]) under ideal conditions. There are at least two reasons for these results. One is related to the asymmetric heating by the plasma jet. This effect enhances the possibility of creating a higher hardness in the hottest end of the heated cylinder when it is quenched. A second reason for the asymmetry in hardness is that the "low mass" end of the part could be quenched faster than the "high mass" end because the quenchant injection port was not located directly below the geometric center of the heated specimen. Therefore, due to the location of this quenchant injection port, the asymmetry in hardness would have occurred even if the entire part had been uniformly heated to the same temperature prior to the quenching process. Other details related to the operating parameters used during the processing of this part, as well as the other parts discussed below, are listed in Table 2.

Figure 4 contains the plotted microhardness readings for sample No. 4. The method of collecting this data was identical to that described above with respect to Fig. 3. This sample exhibited a much wider hardened band of material than sample No. 1 (Fig. 3). The main reason for this effect was, most probably, due to the extended period of time used during the preheating phase of this sample. Specifically, sample No. 4 was preheated from ambient temperatures to 870 °C in 10.9 min, but sample No. 1 was preheated through this temperature span in 5.4 min (see Table 2). Therefore, a wider band of material in sample No. 4 became hot enough (due to conduction) to harden effectively during the quenching process.

Figure 5 contains plotted microhardness readings for samples No. 4 and 5. The main difference in the processing of these two samples involved the soaking times at 870 °C. Sample No. 4 was held at 870 °C for 1 min, but sample No. 5 was held at 870 °C for 2 min. Extending the soaking time at 870 °C also increased the width of material that became hot enough to harden effectively during the quenching process. Only the mid-line data for each of these two samples has been plotted in Fig. 5 to help in clarifying this comparison.

Figure 6 contains plotted microhardness readings for samples No. 4 and 6. The main difference in the processing of these samples involved the quenchant fluid impingement rate. Sample No. 4 was fluid quenched at the rate of 26 l/min, but sample No. 6 was quenched at the rate of 190 l/min. Because sample No. 6 was also heated to 870 °C more rapidly than sample No.

4, the main reason for the wider band of hardened material in sample No. 6 must have been due to the higher quenchant fluid impingement rate. In addition to comparing sample No. 6 and 4, if one also compares sample No. 5 and 6 (see Fig. 5 and 6), it may be seen that the microhardness profiles are nearly identical. This indicates that a longer processing time (*i.e.*, 10.2 min) and lower fluid quenchant rate (*i.e.*, 26 l/min) may be capable of producing nearly the same results as a slightly shorter processing time (*i.e.*, 7.0 min) and higher fluid quenchant rate (*i.e.*, 190 l/min). However, because the cost of using this type of process is almost directly proportional to total run time, the most efficient processing sequence (from an operational cost standpoint) is the one that is the shortest.

5 Conclusion

This experimental study has demonstrated that relatively large, high-carbon E52100 grade steel cylinders can be selectively hardened using a high-power plasma heating system and an appropriate rapid quenching system. Although this phenomenon may not be particularly surprising, the results of this study place some of this behavior on a quantitative basis. Specifically, using the techniques described herein, hollow cylindrical specimens of E52100 steel could be selectively hardened from about 10 HRC to at least 60 HRC in regions directly heated by a plasma jet. Regions adjacent to those directly heated were also hardened, but not as effectively. Therefore, selective hardening within a single part was achieved. The smooth transition in hardness, within the specimens tested during this study, may lead to significant advantages with regard to fatigue-type failures if certain equipment and machinery components can also be selectively hardened in this way. In addition to the E52100 hardening results, a large and effective plasma heating system, which may be useful in more extensive plasma processing studies, has also been described in detail.

Acknowledgment

The experimental assistance of M. Pizzo, throughout the course of this work, is gratefully acknowledged. The assistance of E. Spellman in machining selected components of the plasma jet system, described in this article, is also gratefully acknowledged.

References

1. P.M. Unterweiser, H.E. Boyer, and J.J. Kubbs, Ed., *Heat Treater's Guide*, ASM, Metals Park, 204 (1985).
2. R.J. Kar, R.M. Horn, and V.F. Zackay, *Metall. Trans.*, *10A*(11), 1711-1717 (1979).
3. K. Nakazawa and G. Krauss, *Metall. Trans.*, *9A*(5), 681-689 (1978).
4. H.E. Boyer, *Practical Heat Treating*, ASM, Metals Park, 131 (1984).
5. D. Wang, H. Hua, M.E. Fine, and H.S. Cheng, *Mater. Sci. Eng.*, *A118*, 113-120 (1989).
6. J.M. Beswick, *Metall. Trans.*, *20A*(10), 1961-1973 (1989).
7. C.A. Stickels, *Wear*, *98*(1-3), 199-210 (1984).
8. C.A. Stickels and A.M. Janotik, *Metall. Trans.*, *11A*(3), 467-473 (1980).
9. F.W. Giacobbe, U.S. Pat. No. 4,872,926 (1989).
10. F.W. Giacobbe, *High Temp. Technol.*, *8*(1), 3-8 (1990).
11. F.W. Giacobbe, *High Temp. Technol.*, *7*(1), 11-16 (1989).
12. Corning Technical Bulletin, Macor Machinable Glass Ceramic, Corning Glass Works, Corning, NY.
13. D.S. Clark and W.R. Varney, *Physical Metallurgy for Engineers*, 2nd ed., American Book Co., New York, 143-146 (1969).
14. G. Krauss, *Principles of Heat Treatment of Steel*, ASM, Metals Park, 129 (1985).